A new source of ammonia and carboxylic acids in cloud water: The first evidence of photochemical process involving an iron-amino acid complex

Aurélie Marion, Marcello Brigante, Gilles Mailhot

▶ **To cite this version:**

Aurélie Marion, Marcello Brigante, Gilles Mailhot. A new source of ammonia and carboxylic acids in cloud water: The first evidence of photochemical process involving an iron-amino acid complex. Atmospheric Environment, 2018, 195, pp.179-186. 10.1016/j.atmosenv.2018.09.060 . hal-01985904

HAL Id: hal-01985904
https://hal.science/hal-01985904

Submitted on 17 Dec 2020

HAL is a multi-disciplinary open access archive for the deposit and dissemination of scientific research documents, whether they are published or not. The documents may come from teaching and research institutions in France or abroad, or from public or private research centers.

L'archive ouverte pluridisciplinaire **HAL**, est destinée au dépôt et à la diffusion de documents scientifiques de niveau recherche, publiés ou non, émanant des établissements d'enseignement et de recherche français ou étrangers, des laboratoires publics ou privés.

A new source of ammonia and carboxylic acids in cloud water: The first evidence of photochemical process involving an iron-amino acid complex

Aurélie Marion[a], Marcello Brigante[a*], Gilles Mailhot[a]

[a] Université Clermont Auvergne, CNRS, SIGMA Clermont, Institut de Chimie de Clermont-Ferrand, F-63000 Clermont–Ferrand, France.

[*]Corresponding author : marcello.brigante@uca.fr

Abstract

In the present study we investigate the photochemical properties and impact on cloud water of ferric-aspartate complex (Fe(III)−Asp) under irradiation. Fe(III)−Asp complex was investigated as proxy of ferric-amino acids complexes that could be expected to be present in cloud water. First, the fate of complex under monochromatic (313 and 365 nm) and polychromatic ($\lambda \geq 290$ nm) irradiation is investigated and formation quantum yields of Fe^{2+} are determined. Moreover, hydroxyl radical quantification in the presence of hydrogen peroxide is investigated at cloud water relevant concentrations and under irradiation. Obtained results suggest that hydroxyl radical formation rates are expected to be lower than those obtained considering all iron as aquacomplex or complexed with oxalate. Finally, a phototransformation mechanism for inorganic and organic products formation such as ammonia, malonic, oxalic and formic acids is proposed.

Keywords : Photochemistry, atmospheric water, oxidative capacity, iron complexes

1. Introduction

The atmosphere is a complex medium in which atmospheric particles (liquid and solid) are in continuous interaction with the gas phase. In addition to their direct effect on human health and environmental modifications, atmospheric particles are able to absorb and scatter solar radiation modifying the Earth's radiation budget (Papadimas et al., 2012; Singh et al., 2016; Zhang et al., 2017). Between the compartments of the atmosphere, cloud water droplets have attracted the attention of numerous researchers working in the field of physical-chemistry. In fact, cloud droplets can be considered as a multiphase reactor in which inorganic and organic constituents interact through numerous chemical and photochemical processes (Charbouillot et al., 2012). During the last decade, it has been clearly demonstrated that reactivity of cloud aqueous phase can impact the oxidative budget of the atmosphere. Between the oxidative species present in cloud water, hydroxyl radical ($HO^{\bullet}$) is considered as the most important radical due to the ability to oxidize numerous organic constituents (Gligorovski et al., 2015; Herrmann, 2003; Herrmann et al., 2010). In the past few years, $HO^{\bullet}$ quantification became of great interest to estimate the life-time of organic compounds and numerous spectroscopic and chromatographic approaches have been developed. In the gas phase, the photolysis of ozone can produce electronically excited oxygen atom $O(^1D)$ which can then react with water to form hydroxyl radicals. Once in the gas phase, $HO^{\bullet}$ can be transferred to aqueous phases (Henry's law constant $K_H = 3.0 \pm 0.2$ M atm^{-1}) (Hanson et al., 1992; Mozurkewich, 1995) However, these two possible sources cannot completely explain the concentration of hydroxyl radical in cloud water (also considering the strong reactivity of this radical with organic compounds). In fact, a scarce number of studies measured the production of hydroxyl radicals in cloud water (Arakaki and Faust, 1998; Faust and Allen, 1993) and information on the

oxidizing capacity of cloud water in terms of quantification of $HO^{\bullet}$ and chemical sources is still a subject of debate. Between the different cloud water constituents, hydrogen peroxide (H_2O_2), through its photolysis, is considered as one of the most important sources of $HO^{\bullet}$ (Herrmann et al., 2010; Yu and Barker, 2003). Iron reactivity also contributes to the production of $HO^{\bullet}$ in atmospheric aqueous phases upon Fe(III) photolysis and Fenton reaction (Deguillaume et al., 2005; Faust and Hoigné, 1990; Millero et al., 1991). However, organic constituents of cloud water such as short-chain carboxylic acids and siderophores are able to generate stable complexes with iron modifying the photoreactivity and as consequence the hydroxyl radical formation efficiency (Faust and Zepp, 1993; Long et al., 2013; Passananti et al., 2016; Weller et al., 2014). In fact, the contribution of iron species (as aquacomplexes or organic complexes) to the formation of hydroxyl radical is still a subject of debate (Bianco et al., 2015).

Recently, the presence of amino acids ranging from nM to few µM concentrations has been reported in cloud water collected at the top of puy de Dôme (France) (Bianco et al., 2016). Their contribution to the dissolved organic matter has been estimated to be up to ~ 9% and, considering the high stability constant with ferric ions reported in literature, the presence of stable iron-complexes could be expected (Perrin, 1959).

In the first part of this paper, we investigate the photoreactivity of Fe(III)-aspartic acid complex as probe for iron-amino acid complexes. Aspartate diaion (Asp) was taken into account due to the presence in cloud water and the strong stability constant of complex with ferric ion (log K = 11.4) (Perrin, 1958). The photostability of Fe-Asp complex, considering stability constants reported in literature, is investigated using UV-vis spectroscopy under monochromatic and polychromatic irradiation. Quantum yields of ferrous ions and hydroxyl radical formation rates are determined in the presence or not of hydrogen peroxide to assess the possible impact of iron-aspartate complex photolysis on the oxidative budget of cloud

water. Moreover a phototransformation mechanism leading to the formation of short-chain carboxylic acid and ammonia under polychromatic irradiation is proposed.

2. Material and methods

2.1 Chemicals

All chemicals were used without additional purification: Fe(III)-perchlorate (99.9 %), aspartic acid (99.0 %), malonic acid (99 %), ascorbic acid (99.8 %), coumarin (99 %), 7-hydroxycoumarin (99 %), sodium hydroxide (99.9 %), perchloric acid (70 %), and hydrogen peroxide were purchased from Sigma Aldrich. Ferrous perchlorate (99 %), ferrozine (97 %), sodium formate (99 %) were purchased from Fluka. Ammonium oxalate (99 %) was purchased from Prolabo. All solutions were prepared in water purified by a Millipore milli-Q device (Millipore αQ, resistivity 18 MΩ cm, DOC < 0.1 mg L^{-1}).

2.2 Complex preparation and spectroscopic characterisation

Fresh solutions of Fe-Asp complex are prepared before each experiment by mixing appropriate volumes of $Fe(ClO_4)_3$ and aspartate stock solutions (each 10 mM). The natural pH of mixture was 3.7 and was adjusted using sodium hydroxide if necessary.

In Figure 1 UV-vis spectrum of Fe^{3+}, Asp and Fe-Asp (100 µM + 200 µM) solutions in milli-Q water at pH 3.7 are presented showing the overlap with lamp emission spectra (see irradiation experiments description). Complex speciation is predicted using Hyperquad Simulation and Speciation (HYSS2009) software (Alderighi et al., 1999). Hydrogen peroxide was added to the solution just before each experiment in order to avoid a dark reactivity in the presence of iron (*i.e.* Fenton reaction).

2.3 Irradiation Experiments

Photochemical experiments are performed under monochromatic and polychromatic irradiation to investigate the Fe-complex disappearance and formation of ferrous ions, hydroxyl radicals and transformation products. For monochromatic irradiation, the procedure is the following: 3 mL of solution are irradiated in a quartz cuvette (Hellma QS) under monochromatic light (313 and 365 nm) using a Hg 200W lamp (Oriel) equipped with a monochromator. At fixed interval time the cuvette is transferred into a Varian Carry 300 UV-vis spectrophotometer to follow the time evolution of UV-vis spectra. The radiation fluxes reaching the solution at 313 and 365 nm are respectively 516 and 1230 μW cm^{-2}. Sun-simulated irradiations are performed in homemade photochemical reactor equipped with four fluorescent lamps (Sylvania Blacklight F15W/350BL) with emission from 290 to 450 nm (centered at 350 nm).

To investigate the photochemical behavior under polychromatic radiation, 250 mL of solution are irradiated in a jacked cylindrical reactor (length = 10 cm, volume = 30 mL) thermostated at 283 ± 2 K using a circulation cooling system under aerated conditions. The total irradiance reaching the solution in the UV region (290-400 nm) is equal to 1.27 mW cm^{-2} that is closed to the value measured in a sunny day in Clermont-Ferrand (France) (1.23 mW cm^{-2}) (see Figure 1)

The emission spectra of the irradiation systems (monochromatic and polychromatic) reaching the solution surface are recorded using an optical fiber with a charge coupled device (CCD) spectrophotometer (Ocean Optics USD 2000 + UV–vis) which is calibrated using a DH-2000-CAL Deuterium Tungsten Halogen reference lamp.

2.4 Ferrous ions, hydroxyl radical formation yields and transformation products identification

Ferrous ions (Fe^{2+}) formation is determined using ferrozine complexing agent and detection of complex is performed at 562 nm (ε_{562nm} = 27900 M^{-1} cm^{-1}) (Stookey, 1970) using a Cary

300 UV-vis spectrophotometer.

Hydroxyl radical formation is determined using coumarin as trapping molecules that leads to the formation of stable 7-hydroxycoumarin (7OHC) as high fluorescence product (λ_{ex}= 325 nm, λ_{em} = 456 nm).

Coumarin is added to the solution just before each experiment (a concentration of 500 µM was used to trap all generated hydroxyl radical) and formation of 7OHC is monitored by transferring an aliquot of solution to the spectrofluorometer at fixed interval times. For dark reactivity, coumarin is spiked in a quartz cell previously filled with Fe(III)-Asp^+ + H_2O_2 solution. 7OHC formation at different times is directly monitored by putting the cell inside the spectrofluorimeter.

7OHC formation yield (Y_{7OHC}) is determined following by HPLC coumarin disappearance and formation of 7OHC using Fenton-like reaction (Fe(III) + H_2O_2) as source of hydroxyl radical. The experiment, presented in Figure SM3, is repeated 4 times at pH 3.7 and 283K. 7OHC formation yield is then estimated as the ratio between formation rate of 7OHC and degradation rate of coumarin for each experiment and an average yield of Y_{7OHC} is determined to be 4.6±0.5 %. Considering the reactivity constant of hydroxyl radical with coumarin and aspartate (2×10^9 $M^{-1}s^{-1}$ and 7.5×10^7 $M^{-1}s^{-1}$ respectively) (Buxton et al., 1988; Gopakumar et al., 1977) we can estimate that under experimental conditions (highest aspartate concentration of 200 µM and 0.5 mM of coumarin) about 98.5% of photogenerated hydroxyl radicals react with our probe.

The quantum yield of ferrous ions formation is defined as the ratio between the number of ferrous ions formed and the number of absorbed photons during the same period of time. This value gives an estimation of the photochemical process efficiency. In our experiments iron-aspartate complex is the only absorbing specie present in water and the polychromatic

quantum yield formation of Fe(II) ($\phi_{Fe(II)}$) can be estimated in the overlap range 290-400 (λ_1 and λ_2) by (eq 1).

$$\phi_{Fe(II)} = \frac{R^{f}_{Fe(II)}}{I_a} \quad \text{eq 1}$$

where $R^{f}_{Fe(II)}$ is the Fe(II) formation rate (M s^{-1}) and I_a is the absorbed photon flux per unit of surface and unit of time in the wavelength range by iron-complex. The latter was calculated from eq 2:

$$I_a = \int_{\lambda_1}^{\lambda_2} I_0(\lambda)\,(1-10^{-\varepsilon(\lambda) l [Fe(III)-Asp]})\,d\lambda \quad \text{eq 2}$$

Where I_0 is the incident photon flux, ε the molar absorption coefficient of iron-aspartate, l the optical path length inside the cell or the reactor and [Fe(III)-Asp] the initial complex concentration.

Ion chromatography (IC) analysis is performed using a Dionex DX-320 apparatus with a KOH gradient elution and equipped with an IonPac AG11 (guard column 4 × 50 mm) and an IonPac AS11 (analytical column 5 × 250 mm) for anions and Dionex ICS-1500 equipped with an IonPac CG16 (guard-column 4 × 50 mm) and an Ion-Pac CS16 (analytical column 5 × 250 mm) and a metasulfonic acid (MSA) solution as eluent with an isocratic elution for cations.

2.5 Laser flash photolysis

The laser flash photolysis system has been previously described (Brigante et al., 2010) and the only difference is that the current experiments used the fourth harmonic (λ_{exc} = 266 nm) for the excitation (the energy is set to 50 mJ/pulse). An appropriate volume of chemical stock solutions (Fe^{3+} and aspartate) is mixed just before each experiment to obtain the desired mixtures and concentrations. All experiments are performed at ambient temperature (293 ± 2 K) and in aerated solutions at pH 3.7±0.2.

2.6 Phototransformation experiments

To assess the impact of hydrogen peroxide on the Fe(III)-Asp complex phototransformation, different irradiation experiments are performed in the presence or not of H_2O_2.

5 µM of ferric ions are mixed to 200 µM of aspartate before irradiation. The amount of aspartate needed was determined using Hyperquad Simulation and Speciation (HYSS2009) software in order to obtain more than 90% of Fe(III)-Asp^+ complex in solution. Three experiments are performed: with the presence of Fe(III)-Asp complex in the absence or presence of H_2O_2. Moreover, to identify the mechanism in the presence of H_2O_2, additions of ferric ions or H_2O_2 are performed after 240 min of irradiation.

The disappearance of Fe(III)-Asp complex is followed by measuring the absorption at 289 nm while concentration of ferrous ions is determined using the ferrozine method previously described while ammonium ions are quantified with ionic chromatography.

3. Results and Discussion

3.1 Complex formation and phototransformation yields

Stability constants of complexes between ferric ion and amino acids have been reported in literature (Perrin, 1958) suggesting the formation of stable complex with a stoichiometry 1:1. High stability constant was found for aspartic acids (logK of 11.4). Vukosav and Mlakar (Vukosav and Mlakar, 2014) investigated the ferric and ferrous ions complexation with an excess of aspartic acid using square wave voltammetry. The authors reported the formation of different iron-aspartate complexes as function of solution pH. In our work, stability constants reported in Table SM1 are used to predict the iron-aspartate complex form under our experimental conditions. In Figure SM1 different forms of iron complexes are reported as function of pH considering 100 µM of Fe(III) and aspartate concentration ranging from 50 to 300 µM. Two main complexes between Fe(III) and aspartate are found : Fe(III)−$HAsp^{2+}$ and

Fe(III)−Asp^+. They both have a stoichiometry ratio of 1:1 and are complexes between Fe^{3+} and respectively aspartate monoanion (HL^-) and aspartate dianion (L^{2-}). The latter is expected to be formed increasing the pH in which L^{2-} is the predominant specie (pKa ~3.8) (Rakhimova et al., 2013). In the presence of aspartate concentration greater than Fe(III), the main specie present in solution at pH 3.7 (natural pH) is Fe(III)−Asp^+ complex. However, at molar ratio 1:1, ferric ion is partially present as aquacomplex ($Fe(OH)^{2+}$ and $Fe(OH)_2^+$). Increasing the concentration of aspartate (ratio 1:2), about 92% of iron is present as Fe(III)−Asp^+ and no more Fe(II)-aquacomplexes are present. Moreover, no significant difference in the iron speciation can be appreciated using higher ratio (1:3).

Laser flash photolysis experiments are performed using Fe(III) mixed with aspartate solutions and amount of ferric ions disappearance is monitored following the absorption decrease at 290 nm. Iron bleaching is monitored upon 266 nm excitation of iron and iron-aspartate solutions producing a transient spectrum reported in Figure 2A. Interestingly, when experiments are performed in the presence of aspartate high decay is observed at ~290 nm (see insert of Figure 2A) indicating a different photoreduction efficiency of Fe(III) in the presence of amino acid. Absorption decay at 290 nm of Fe(III) [100 μM] solution in the presence of different aspartate concentrations (Figure 2B) also indicates a non-linearity of experimental data fit with a plateau value observed near the ration [Asp]/[Fe(III) = 2.0. For these reasons the next experiments are performed with 100 μM Fe(III) and 200 μM Asp which correspond to the formation of almost 100 μM of Fe(III)−Asp^+ complex.

Under monochromatic (313 and 365 nm) and polychromatic (290-450) irradiation, the UV-vis spectrum of Fe(III)−Asp^+ undergoes a fast decrease, and after about 5 min of irradiation at 365 nm, about 15 % of the complex disappeared (see Figure SM2). Measurements of ferrous ions in solution confirm that photolysis of Fe(III)−Asp^+ complex leads to the quantitative photoreduction of Fe(III) into Fe(II) and consequent oxidation of ligand following a well-

known ligand-to-metal charge transfer reaction (LMCT) as reported in reaction (R1).

$$Fe(III) - Asp^{+} \xrightarrow{h\nu} Fe(II) + Asp^{\bullet -} \qquad \text{(R1)}$$

In Figure 3 the disappearance of complex monitored at 290 nm and formation of ferrous ions under polychromatic irradiation are displayed. Similar degradation and formation rates for Fe(III)−Asp^{+} and Fe^{2+} (respectively $R^{d}_{Fe(III)-Asp^{+}}$ = (3.79 ± 0.33) × 10^{-6} M min^{-1} and $R^{f}_{Fe^{2+}}$ = (3.71 ± 0.23) × 10^{-6} M min^{-1}) are determined indicating that ferrous ions are stable in water despite a possible oxidation into ferric ions observed at pH higher than 4.0 (Morgan and Lahav, 2007). Direct hydroxyl radical formation has been observed during iron-aquacomplexes photolysis while photolysis of iron-organic complexes is suggested to lead to the formation of reactive oxygen species (ROS). Reactivity of dissolved oxygen with organic ligand radical ($Asp^{\bullet}$) can lead to the formation of superoxide radical anion ($O_2^{\bullet -}$) that can react with iron complex or, through disproportionation, leads to the formation of hydrogen peroxide (Bielski and Allen, 1977; Wang et al., 2009; Zhang et al., 2009). Hydrogen peroxide can react with ferrous ions in solution generating hydroxyl radical (Fenton reaction). Formation of hydrogen peroxide has been also demonstrated during photolysis of Fe(III)-oxalate complexes through oxidation of Fe(II) into Fe(III) by $HO_2^{\bullet}/O_2^{\bullet -}$ (Zuo, 1995).

Zhang and coworkers determined that photolysis quantum yield of Fe(III)-pyruvate complex at 355 nm decreases from 1.0 to 0.46 in deoxygenated and aerated solutions respectively (Zhang et al., 2009). This result demonstrates the key role of molecular oxygen on the Fe(II)/Fe(III) catalytic process in agreement with formation of hydroperoxide/superoxide radical and finally hydrogen peroxide. However, quantification of hydrogen peroxide in solution is difficult due to the fast reactivity with photogenerated ferrous ions. Under polychromatic irradiation ferrous ions formation from 100 µM of Fe(III)−Asp^{+} solution is presented in Figure 4 and compared to the data obtained from 100 µM of Fe(III)-aquacomplex ($Fe(OH)^{2+}$) and iron-monoxalate complex (Fe(III)−$(C_2O_4)^{+}$). The pH of the solutions is the

natural pH : respectively 3.8±0.1 for Fe(III)-Asp+ and $Fe(OH)_2^+$ solutions and 2.6±0.1 for Fe(III)−$(C_2O_4)^+$ solution. Under 290-450 nm irradiation Fe^{2+} formation rate ($R^f_{Fe^{2+}}$) for Fe(III)−Asp^+ is (3.79 ± 0.33) ×10^{-6} M min^{-1} while a rate of (4.99 ± 1.43) ×10^{-7} M min^{-1} and (2.50 ± 0.17) ×10^{-5} M min^{-1} is determined for $Fe(OH)^{2+}$ and Fe(III)−$(C_2O_4)^+$ respectively.

In Table 1 Fe^{2+} formation quantum yields are reported and compared with previously investigated iron complexes adopted as proxies for Fe-complexes in cloud water. Ferrous ions formation yield from Fe(III)−Asp^+ complex is about 5 times lower than the value measured for Fe(III)−$(C_2O_4)^+$ under the same irradiation conditions. By complexing with organic ligands, Fe(III) photolysis is faster than for the aquacomplex form. This leads to higher Fe^{2+} formation rates which modify the speciation of iron in the aqueous phase of cloud and therefore the iron cycle in clouds.

3.2 Hydroxyl radical formation

In order to assess the impact of Fe(III)−Asp^+ complex photolysis on the oxidative capacity and chemical composition of cloud water, different experiments by varying the initial concentration of complex and presence of hydrogen peroxide are performed under dark and polychromatic irradiation as summarized in Table 2. Hydroxyl radical formation rate ($R^f_{HO\bullet}$) is quantified spiking the solution with 500 µM of coumarin that quantitatively trap all generated hydroxyl radical ($k_{coumarin,HO\bullet}$ = 6.4×10^9 M^{-1} s^{-1}) (Singh et al., 2002) generating a fluorescent intermediate (7-OH-coumarin, 7OHC).

In dark experiments no relevant formation of hydroxyl radical is observed for all experiments excepted for experiment 2 and 4 in which a formation rate of hydroxyl radical ($R^f_{HO\bullet}$) of (2.30 ± 0.12) × 10^{-8} and (2.98 ± 0.12) × 10^{-8} M min^{-1} is determined. Under polychromatic irradiation (Figure 5), a similar formation rate of hydroxyl radical is observed for experiment

1 and 3 (ferric ion and Fe(III)-Asp^+ photolysis) with a $R^f_{HO^\bullet}$ of $(1.06 \pm 0.11) \times 10^{-7}$ and $(9.76 \pm 0.44) \times 10^{-8}$ M min^{-1} respectively. In the presence of hydrogen peroxide (1 mM), as expected, an increase of $HO^\bullet$ formation rate is observed up to $(7.18 \pm 0.33) \times 10^{-7}$ M min^{-1} for 100 µM of Fe(III)-Asp^+ complex in the presence of 1 mM of hydrogen peroxide.

3.3 Phototransformation mechanism

The mechanisms of Fe(III)-Asp^+ complex transformation under cloud water conditions is investigated mixing 5 µM of Fe(III) with 200 µM of aspartate and solution was irradiated under sun-simulated conditions. Fe(III) concentration is typical for aqueous phase of clouds and aspartate concentration is estimated thanks to HYSS2009 software to obtain more than 90% of Fe(III)-Asp^+ complex. Under these conditions, almost 5 µM of Fe(III)-Asp^+ are present in solution with an excess of aspartate. In absence of hydrogen peroxide, formations of ammonia (NH_4^+) and ferrous ions are proportional to the disappearance of Fe(III)-Asp^+ complex (Figure 6A) suggesting that irradiation of one complex molecule leads to the reduction of ferric into ferrous ion and quantitative formation of one NH_4^+ through a complex mechanism starting from a first ligand-to metal charge transfer (LMCT) reaction between Fe(III) and Asp.

When the same experiments are performed with addition of 50 µM of H_2O_2 (Figure 6B), an important increase of NH_4^+ is observed leading to a significantly higher concentration than the initial concentration of Fe(III)-Asp^+ complex (about 3 times higher after 100 min of irradiation). Moreover, formation of short-chain carboxylic acids such as malonic, oxalic and formic acids is observed during irradiation (Figure SM4). In absence of hydrogen peroxide, carboxylic acids are not detected in solution suggesting that their formation can be probably attributed to the oxidation of aldehyde that is generated from deamination of aspartic radical. Moreover, no relevant formation of NH_4^+ or carboxylic acids has been noticed in absence of

ferric ions (i.e. only aspartate and hydrogen peroxide).

The addition of 10 µM of ferric ions after 240 min of irradiation shows an important increase of Fe(III)-Asp^+ complex which is again photo-degraded and leads to an important formation of NH_4^+. The increase of ferrous ions concentration is not proportional to the formation of ammonia which suggests a re-oxidation of ferrous ions into ferric ions (Fenton reaction) which is complexed again with the excess of aspartate in solution.

To confirm this hypothesis, the same experiment has been performed with an addition of hydrogen peroxide (200 µM) after 240 min of irradiation. When H_2O_2 is added (Figure 6C), a relevant decrease of Fe^{2+} concentration (about 0.8µM), proportional to the complex formation, is observed confirming a re-oxidation of Fe^{2+} into Fe^{3+} (Fenton reaction) which then is re-complexed by aspartate in solution. The irradiation of this solution highlights an important increase of ammonia concentration despite a quite stable concentration of Fe^{2+} and Fe(III)-Asp^+ complex. In Figure 7, the proposed mechanisms from Fe(III)-Asp^+ is presented indicating that different steps leading to the formation of ammonia from Aspartate radical anion. A first decarbonylation of Aspartate radical anion leads to the formation of amine radical. This latter can react with molecular oxygen leading to the formation of ammonia and aldehyde (R-CHO). The formation of short-chain carboxylic acids observed only in the presence of hydrogen peroxide can be attributed to the hydroxyl radical mediated oxidation of aldehyde as reported in the literature (Charbouillot et al., 2012). These different photoinduced steps lead to the formation of carbon dioxide CO_2 and therefore represent a sink for organic compounds in aqueous phase. As observed for Fe-oxalate, by complexation processes and photoreaction iron is allowing large organic compounds to be transformed into smaller compounds and CO_2.

4. Conclusions

The present work investigate, for the first time of our knowledge, the photochemical reactivity of an Fe(III)-amino acid complex in atmospheric mimic waters. The photolysis of Fe(III)-Asp^{+} complex under sun-simulated conditions leads to the formation of ammonia as main product and short chain carboxylic acid through a more complex degradation mechanism. In the presence of hydrogen peroxide the formation of hydroxyl radical is enhanced leading to the re-oxydation of ferrous into ferric anion during Fenton process and a possible formation of a new complex. The formation of iron-amino acid complexes can represent a degradation pathway for amino acids oxidation as well as new photochemical sources of carboxylic acids and ammonia in cloud aqueous phase. The relevance of this photochemical reactivity needs to be extended to aerosols. In fact, we can expect that the presence of higher amino acids and iron found in atmospheric particles can induce these new heterogeneous processes enhanced by solar irradiation. For these reasons, iron-amino acids photoreactivty can modify the physico-chemical properties of atmospheric particle (*i.e.* hygroscopicity) but also the composition of solid and gas phases of atmosphere.

Acknowledgements

Authors acknowledge financial support from the Regional Council of Auvergne and from the "Fédération de Recherches en Environnement" through the CPER “Environnement” founded by the “Région Auvergne,” the French government, FEDER from the European community, and the ANR BIOCAP (ANR-13-BS06-0004).

References

Alderighi, L., Gans, P., Ienco, A., Peters, D., Sabatini, A., Vacca, A., 1999. Hyperquad simulation and speciation (HySS): a utility program for the investigation of equilibria involving soluble and partially soluble species. Coord. Chem. Rev. 184, 311-318.

Arakaki, T., Faust, B.C., 1998. Sources, sinks, and mechanisms of hydroxyl radical (OH) photoproduction and consumption in authentic acidic continental cloud waters from Whiteface Mountain, New York: The role of the Fe(r) (r = II, III) photochemical cycle. J. Geophys. Res. 103, 3487-3504.

Bianco, A., Passananti, M., Perroux, H., Voyard, G., Mouchel-Vallon, C., Chaumerliac, N., Mailhot, G., Deguillaume, L., Brigante, M., 2015. A better understanding of hydroxyl radical photochemical sources in cloud waters collected at the puy de Dôme station – experimental versus modelled formation rates. Atmos. Chem. Phys. 15, 9191-9202.

Bianco, A., Voyard, G., Deguillaume, L., Mailhot, G., Brigante, M., 2016. Improving the characterization of dissolved organic carbon in cloud water: Amino acids and their impact on the oxidant capacity. Sci. Rep. 6, 37420.

Bielski, B.H.J., Allen, A.O., 1977. Mechanism of the disproportionation of superoxide radicals. J. Phys. Chem. 81, 1048-1050.

Brigante, M., Charbouillot, T., Vione, D., Mailhot, G., 2010. Photochemistry of 1-Nitronaphthalene: A potential source of singlet oxygen and radical species in atmospheric waters. J. Phys. Chem. A 114, 2830-2836.

Buxton, G.V., Greenstock, C.L., Helman, W.P., Ross, A.B., 1988. Critical review of rate constants for reactions of hydrated electrons, hydrogen atoms and hydroxyl radicals (OH/O−) in aqueous solution. J. Phys. Chem. Ref. Data 17, 513-886.

Charbouillot, T., Gorini, S., Voyard, G., Parazols, M., Brigante, M., Deguillaume, L., Delort, A.-M., Mailhot, G., 2012. Mechanism of carboxylic acid photooxidation in atmospheric aqueous phase: Formation, fate and reactivity. Atmos. Environ. 56, 1-8.

Deguillaume, L., Leriche, M., Desboeufs, K., Mailhot, G., George, C., Chaumerliac, N., 2005. Transition metals in atmospheric liquid phases: Sources, reactivity, and sensitive parameters. Chem. Rev. 105, 3388-3431.

Faust, B.C., Allen, J.M., 1993. Aqueous-phase photochemical formation of hydroxyl radical in authentic cloudwaters and fogwaters. Environ. Sci. Technol. 27, 1221-1224.

Faust, B.C., Hoigné, J., 1990. Photolysis of Fe (III)-hydroxy complexes as sources of OH radicals in clouds, fog and rain. Atmos. Environ. 24, 79-89.

Faust, B.C., Zepp, R.G., 1993. Photochemistry of aqueous iron(III)-polycarboxylate complexes: roles in the chemistry of atmospheric and surface waters. Environ. Sci. Technol. 27, 2517-2522.

Gligorovski, S., Strekowski, R., Barbati, S., Vione, D., 2015. Environmental implications of hydroxyl radicals (•OH). Chem. Rev. 115, 13051-13092.

Gopakumar, K., Kini, U.R., Ashawa, S.C., Bhandari, N.S., Krishnan, G.U., Krishnan, D., 1977. Gamma irradiation of coumarin in aqueous solution. Radiat. Eff. 32, 199-203.

Hanson, D.R., Burkholder, J.B., Howard, C.J., Ravishankara, A.R., 1992. Measurement of hydroxyl and hydroperoxy radical uptake coefficients on water and sulfuric acid surfaces. J. Phys. Chem. 96, 4979-4985.

Herrmann, H., 2003. Kinetics of aqueous phase reactions relevant for atmospheric chemistry. Chem. Rev. 103, 4691-4716.

Herrmann, H., Hoffmann, D., Schaefer, T., Bräuer, P., Tilgner, A., 2010. Tropospheric aqueous-phase free-radical chemistry: Radical sources, spectra, reaction kinetics and prediction tools. ChemPhysChem 11, 3796-3822.

Long, Y., Charbouillot, T., Brigante, M., Mailhot, G., Delort, A.-M., Chaumerliac, N., Deguillaume, L., 2013. Evaluation of modeled cloud chemistry mechanism against laboratory irradiation experiments: The HxOy/iron/carboxylic acid chemical system. Atmos. Environ. 77, 686-695.

Millero, F.J., Sotolongo, S., Stade, D.J., Vega, C.A., 1991. Effect of ionic interactions on the oxidation of Fe(II) with H_2O_2 in aqueous solutions. J. Solution Chem. 20, 1079-1092.

Morgan, B., Lahav, O., 2007. The effect of pH on the kinetics of spontaneous Fe(II) oxidation by O_2 in aqueous solution – basic principles and a simple heuristic description. Chemosphere 68, 2080-2084.

Mozurkewich, M., 1995. Mechanisms for the release of halogens from sea-salt particles by free radical reactions. J. Geophys. Res. 100, 14199-14207.

Papadimas, C.D., Hatzianastassiou, N., Matsoukas, C., Kanakidou, M., Mihalopoulos, N., Vardavas, I., 2012. The direct effect of aerosols on solar radiation over the broader Mediterranean basin. Atmos. Chem. Phys. 12, 7165-7185.

Passananti, M., Vinatier, V., Delort, A.-M., Mailhot, G., Brigante, M., 2016. Siderophores in cloud waters and potential impact on atmospheric chemistry: Photoreactivity of iron complexes under sun-simulated conditions.

Environ. Sci. Technol. 50, 9324-9332.
Perrin, D.D., 1958. The stability of complexes of ferric ion and amino-acids. J. Chem. Soc, 3125-3128.
Perrin, D.D., 1959. The stability of iron complexes. Part III. A comparison of 1 : 1 ferric and ferrous amino-acid complexes. J. Chem. Soc, 290-296.
Rakhimova, M.M., Nurmatov, T.M., Yusupov, N.Z., Davlatshoeva, D.A., Ismailova, M.A., Ismatov, A., 2013. Iron aspartate complexes and model processes of their formation. Russ. J. Coord. Chem. 39, 746-750.
Singh, A., Srivastava, R., Rastogi, N., Singh, D., 2016. Absorbing and scattering aerosols over the source region of biomass burning emissions: Implications in the assessment of optical and radiative properties. Atmos. Environ. 127, 61-68.
Singh, T.S., Madhava Rao, B.S., Mohan, H., Mittal, J.P., 2002. A pulse radiolysis study of coumarin and its derivatives. J. Photochem. Photobiol., A 153, 163-171.
Stookey, L.L., 1970. Ferrozine - a new spectrophotometric reagent for iron. Anal. Chem. 42, 779-781.
Vukosav, P., Mlakar, M., 2014. Speciation of biochemically important iron complexes with amino acids: L-aspartic acid and L-aspartic acid - glycine mixture. Electrochim. Acta, 29-35.
Wang, L., Zhang, C., Mestankova, H., Wu, F., Deng, N., Pan, G., Bolte, M., Mailhot, G., 2009. Photoinduced degradation of 2,4-dichlorophenol in water: influence of various Fe(III) carboxylates. Photochem. Photobiol. Sci. 8, 1059-1065.
Weller, C., Tilgner, A., Brauer, P., Herrmann, H., 2014. Modeling the impact of iron-carboxylate photochemistry on radical budget and carboxylate degradation in cloud droplets and particles. Environ. Sci. Technol. 48, 5652-5659.
Yu, X.-Y., Barker, J.R., 2003. Hydrogen peroxide photolysis in acidic aqueous solutions containing chloride ions. II. Quantum yield of $HO_{(Aq)}$ radicals. J. Phys. Chem. A 107, 1325-1332.
Zhang, M., Ma, Y., Gong, W., Wang, L., Xia, X., Che, H., Hu, B., Liu, B., 2017. Aerosol radiative effect in UV, VIS, NIR, and SW spectra under haze and high-humidity urban conditions. Atmos. Environ. 166, 9-21.
Zhang, X., Gong, Y., Wu, F., Deng, N., Pozdnyakov, I.P., Glebov, E.M., Grivin, V.P., Plyusnin, V.F., Bazhinb, N.M., 2009. Photochemistry of the iron(III) complex with pyruvic acid in aqueous solutions. Russ. Chem. Bull. 58, 1828-1836.
Zuo, Y., 1995. Kinetics of photochemical/chemical cycling of iron coupled with organic substances in cloud and fog droplets. Geochim. Cosmochim. Acta 59, 3123-3130.

Conditions	ϕ_{313nm}	ϕ_{365nm}	$\phi_{300-450nm}$
$Fe(III)-Asp^{+}$	0.25±0.04	0.11±0.04	0.31±0.06
Fe^{3+}aquacomplex $(FeOH)^{2+}$	–	0.027 (Wang et al., 2009)	0.03±0.01
$Fe(III)-(C_2O_4)^{+}$	–	–	1.6±0.2
$Fe(III)-(C_2O_4)_2^{-}$	0.10 (Long et al., 2013)	0.085 (Long et al., 2013)	–
$Fe(III)-(H_2C_3O_3)^{2+}$		0.46* (Zhang et al., 2009)	

Table 1: Formation quantum yields of Fe^{2+} under monochromatic (313 and 365 nm) and polychromatic (300-450 nm) irradiation. $Fe(III)-(C_2O_4)^{+}$ and $Fe(III)-(C_2O_4)_2^{-}$ are ferric-mono and di-oxalate complexes respectively while $Fe(III)-(C_3H_3O_3)^{2+}$ refers to ferric-pyruvate species. * the quantum yields is determined at 355 nm

Experiment		Fe(III)(μM)	Asp (μM)	H_2O_2 (μM)	$R^f_{HO^\bullet}$ ($\times 10^{-7}$ M min^{-1})
1	Dark	100	−	−	0.015±0.003
2	Dark	100	−	1000	0.230±0.012
3	Dark	100	200	−	0.017±0.003
4	Dark	100	200	1000	0.298±0.012
1	Light	100	−	−	1.06±0.11
2	Light	100	−	1000	3.47±0.12
3	Light	100	200	−	0.976±0.044
4	Light	100	200	1000	7.18±0.33

Table 2: Initial chemical composition of solutions for experiments under dark and polychromatic irradiation and the corresponding $HO^\bullet$ formation rate $R^f_{HO^\bullet}$. The pH was 3.7 and temperature 283 K

Figure Captions

1) Absorption spectra of Fe^{3+} 100 µM, aspartate 1 mM and Fe^{3+} 100 µM + Asp 200 µM solutions at pH 3.7. Emission spectra of four fluorescent lamps reaching the solution surface and sun spectrum acquired during a spring day at Clermont-Ferrand (France).

2) **A:** Transient absorption spectra produced upon 266 nm excitation of Fe(III) 500 µM solution (○) and Fe(III) 500 µM + aspartate 500 µM solution (●). Solid lines represent the fit of experimental data with a Gaussian equation. Error bars are determined from the signal resolution of absorption decay signal. The insert shows the absorption decay signal monitored at 290 nm. **B:** Absorption decay monitored at 290 nm *vs* ratio [Fe(III)]/[Asp]. Errors bars are determined considering standard deviation of 3 different experiments. Experiments are performed at pH 3.7 ± 0.2, 293 K and aerated conditions.

3) Fe(III)−Asp^+ complex (monitored at 290 nm) disappearance and Fe^{2+} formation under polychromatic irradiation (290-400 nm) of Fe^{3+} 100µM + Asp 200 µM solutions at pH 3.7. Continuous line represents the exponential fit of experimental results, while dashed line the 95% confidence of fit.

4) Fe^{2+} formation during polychromatic irradiation of 100 µM $Fe(OH)^{2+}$, Fe(III)−Asp^+ or Fe(III)−$(C_2O_4)^+$) at pH 3.7 in aerated solutions.

5) Hydroxyl radical formation during polychromatic irradiation of Fe(III) 100 µM in the presence of hydrogen peroxide and/or aspartate.

6) Polychromatic irradiation of (**A**) Fe^{3+} 5µM + Asp 200 µM solution ; (**B**) Fe^{3+} 5µM + Asp 200 µM + 50 µM of H_2O_2 solution with addition of 10µM of Fe^{3+} after 240 min ; (**C**) Same condition as (B) with addition of 200 µM of H_2O_2 after 240 min. The pH of

the solutions was set to 3.7.

7) Mechanism of Fe(III)-Asp^+ photolysis and formation of main products.

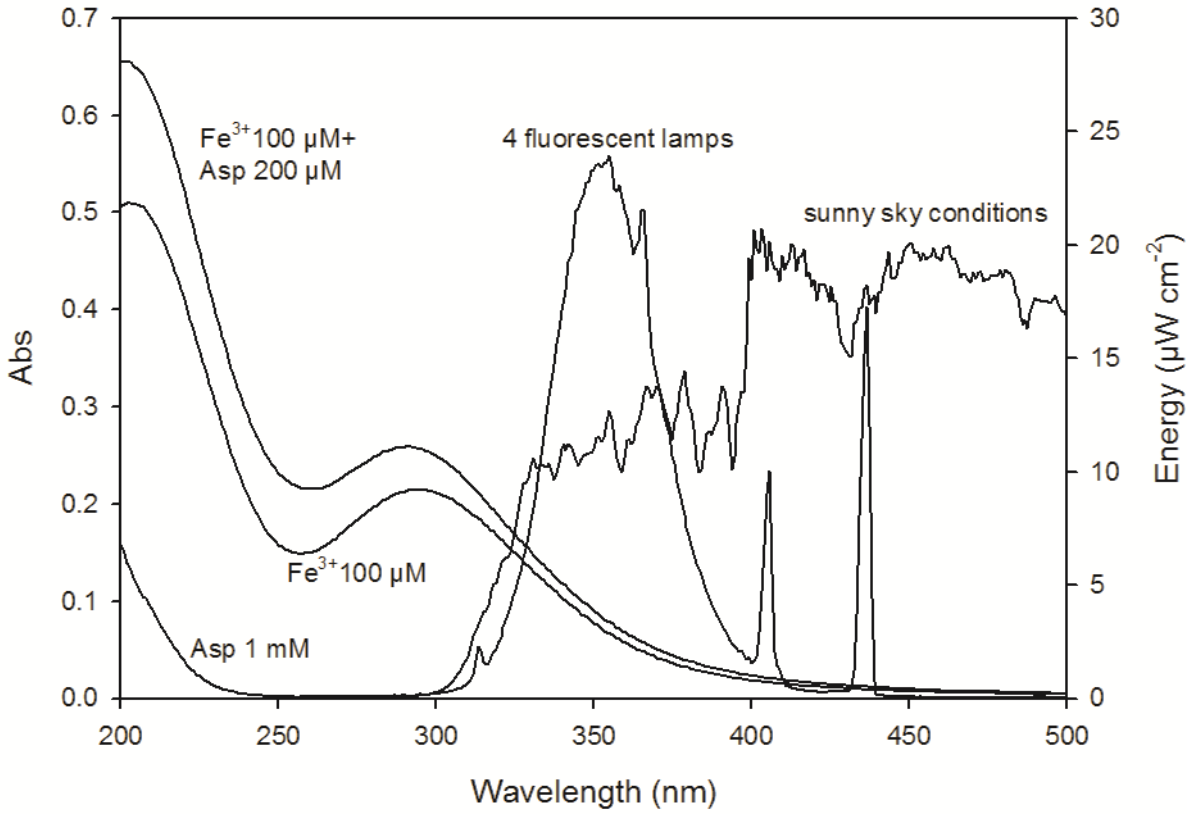

474

475 **Figure 1**

476

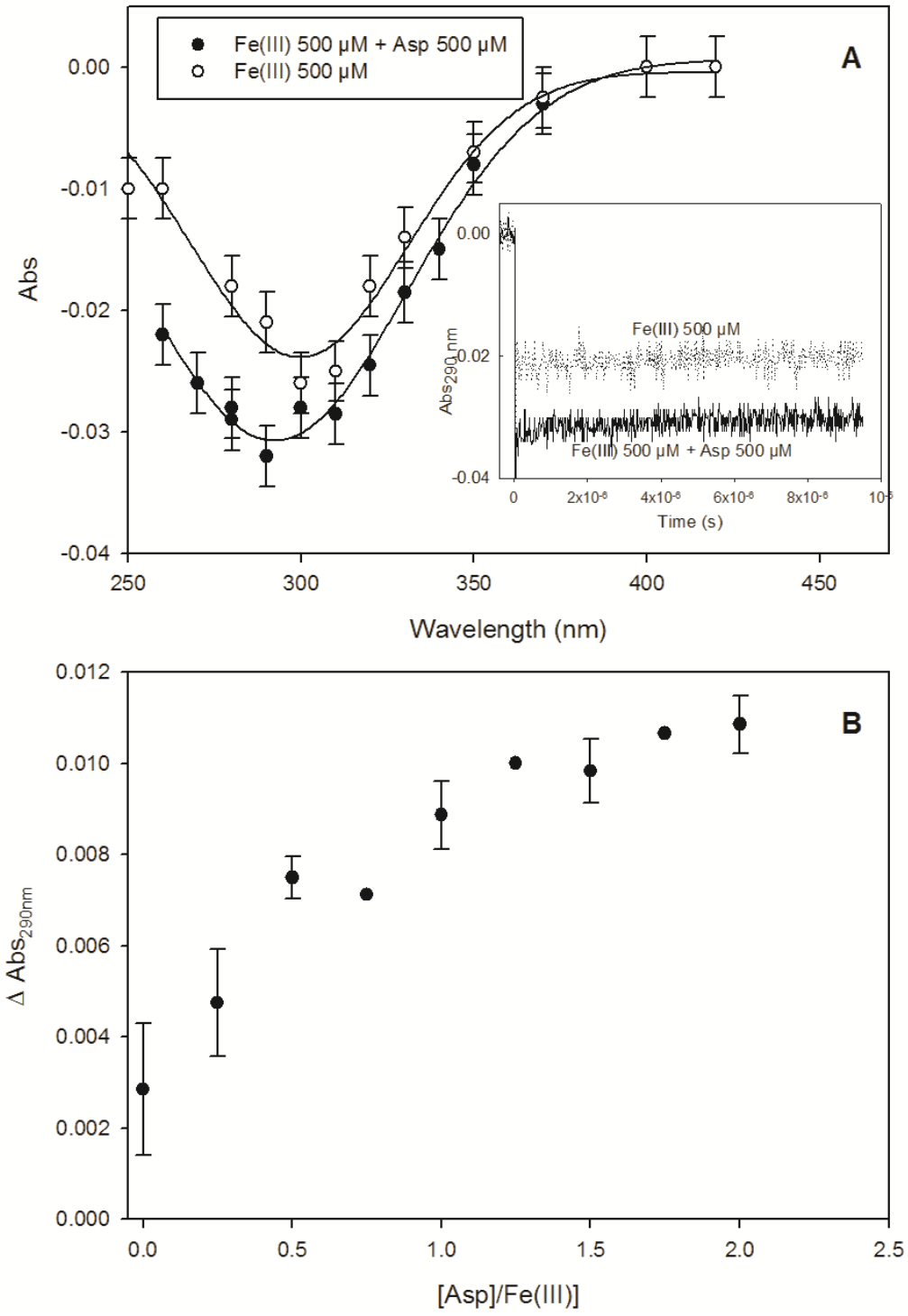

477

478 **Figure 2**

479

480

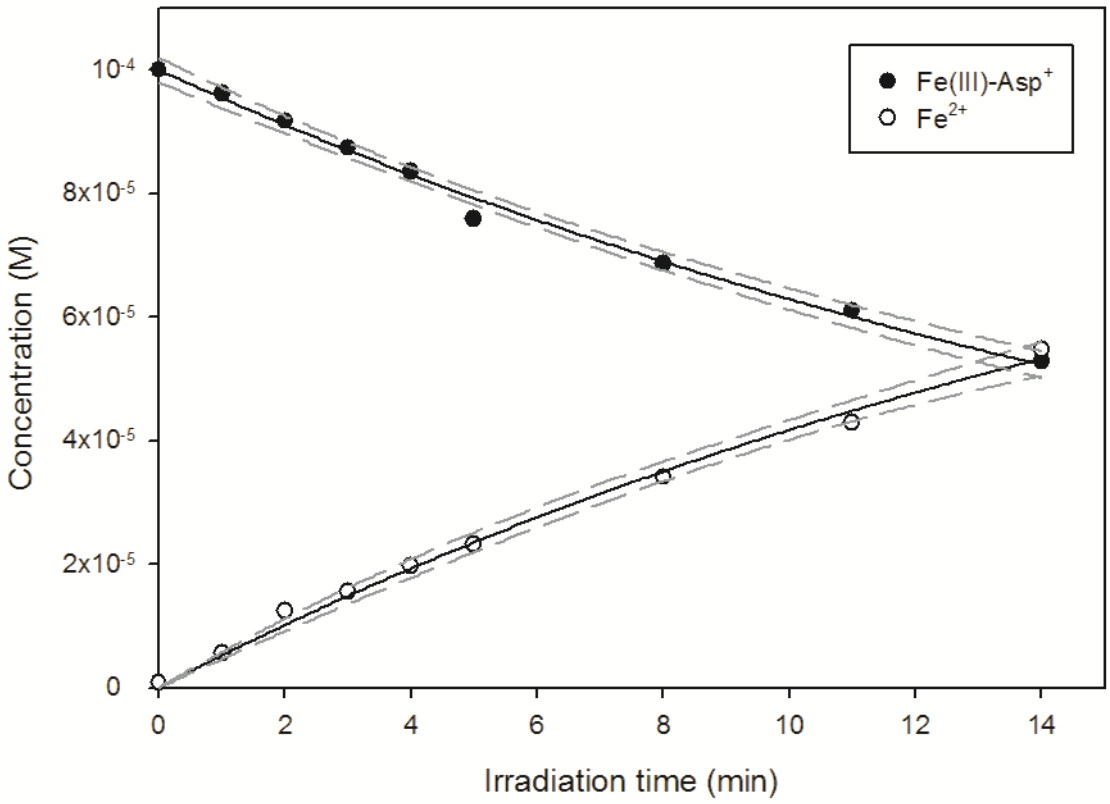

481

482 **Figure 3**

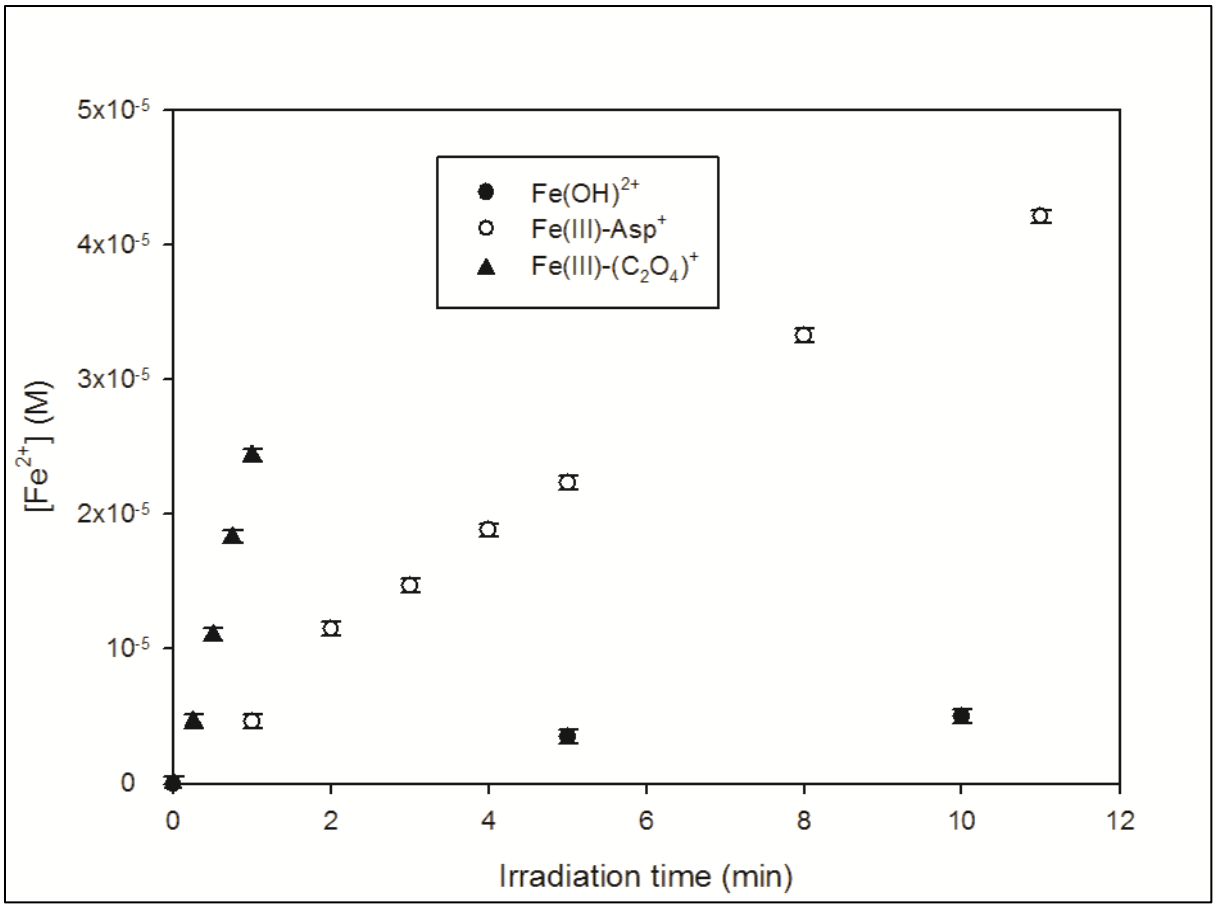

483

484 **Figure 4**

485

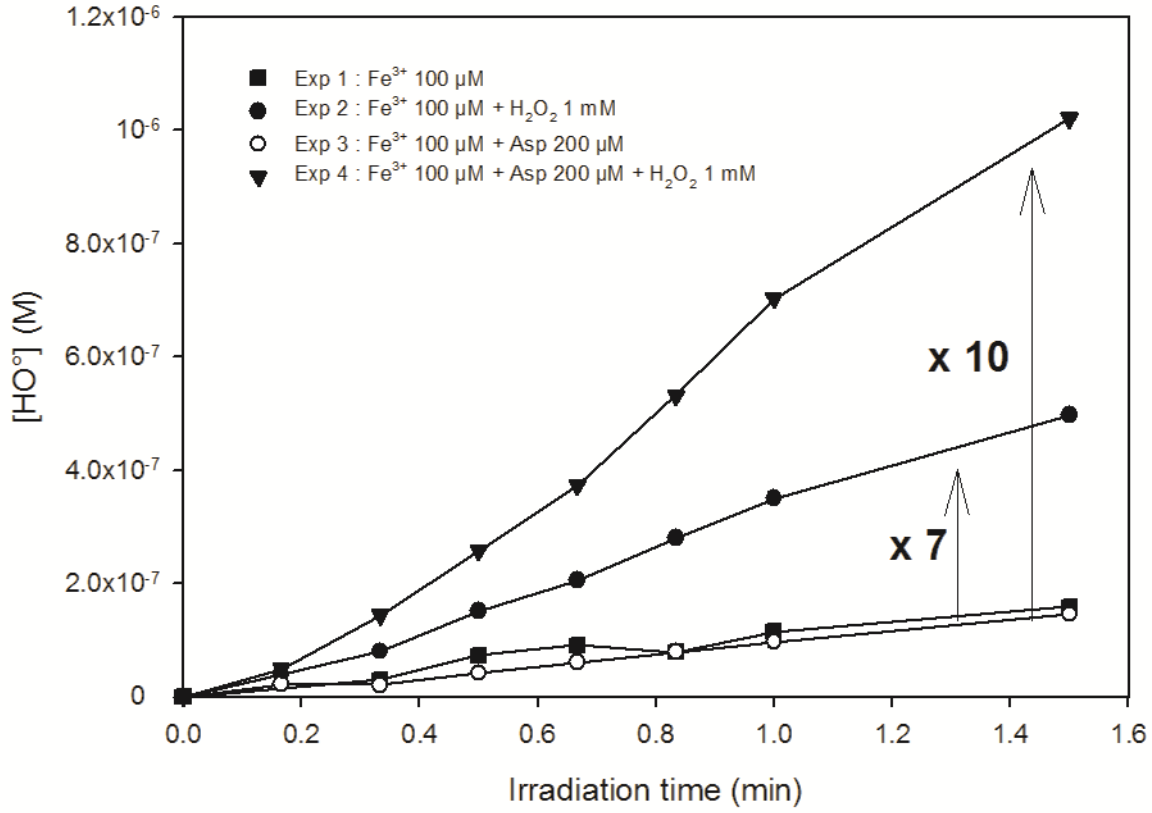
1.2x10-6
10-6
8.0x10-7
6.0x10-7
4.0x10-7
2.0x10-7
0
[HO°] (M)
Exp 1 : Fe3+ 100 µM
Exp 2 : Fe3+ 100 µM + H2O2 1 mM
Exp 3 : Fe3+ 100 µM + Asp 200 µM
Exp 4 : Fe3+ 100 µM + Asp 200 µM + H2O2 1 mM
x 10
x 7
0.0
0.2
0.4
0.6
0.8
1.0
1.2
1.4
1.6
Irradiation time (min)

Figure 5

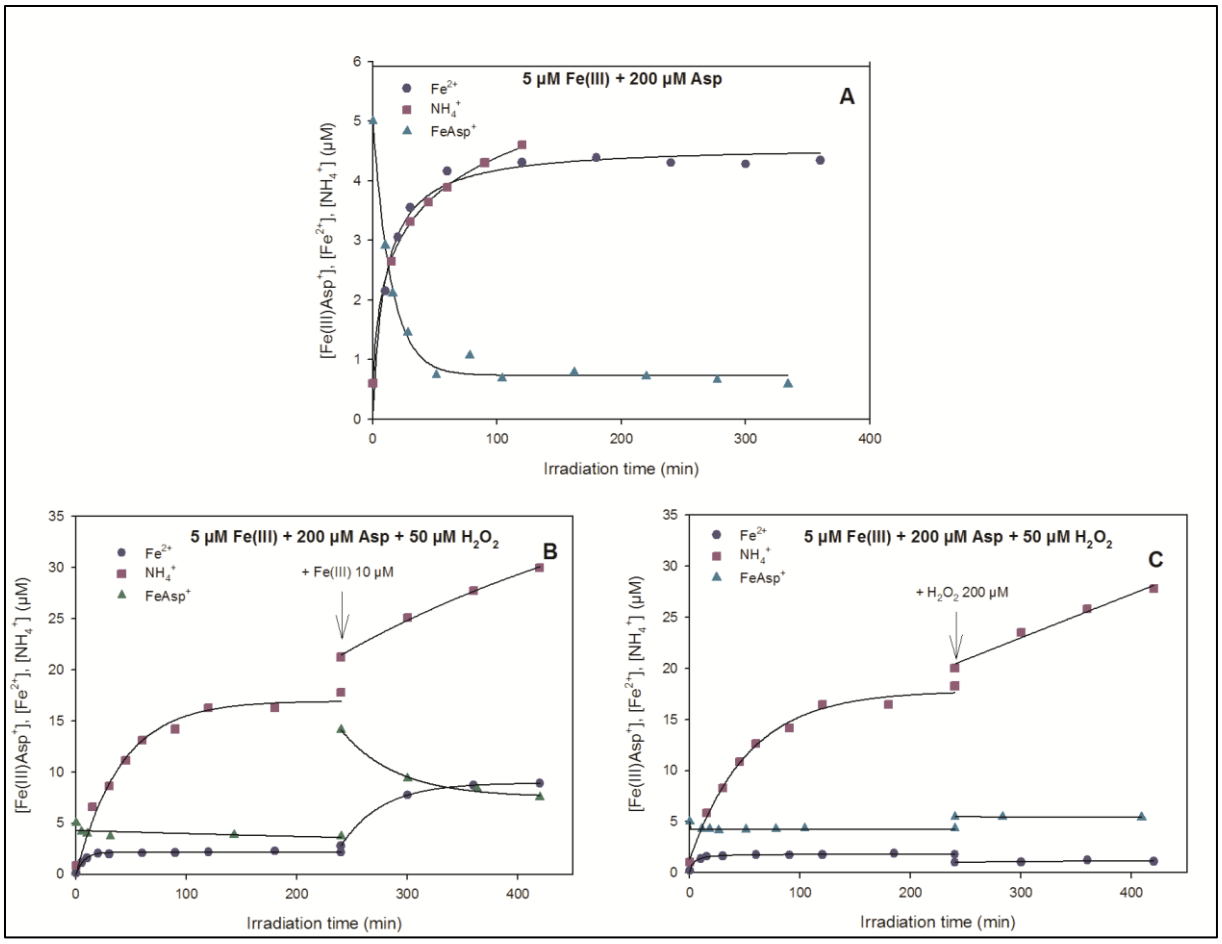

491

492 **Figure 6**

493

494

495

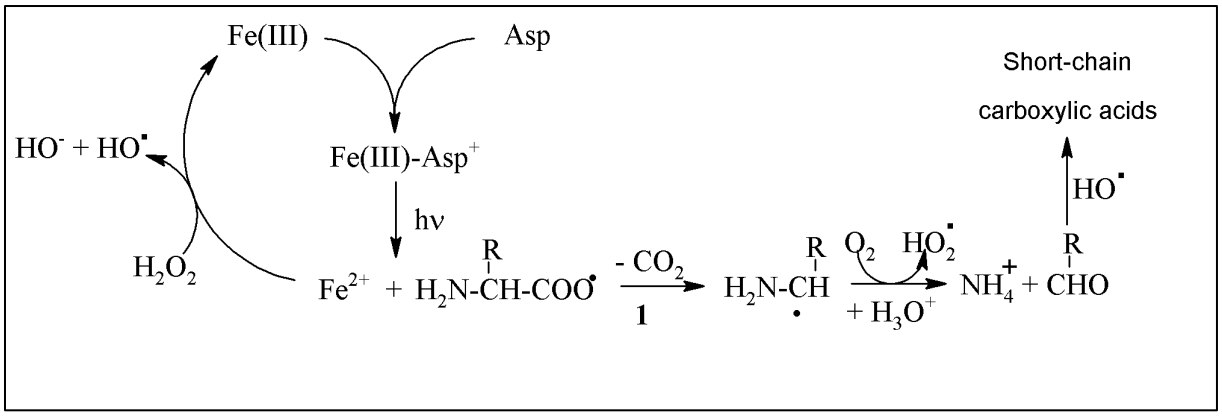
Fe(III)
Asp
Short-chain
carboxylic acids
HO⁻ + HO•
Fe(III)-Asp⁺
hν
HO•
H2O2
R
Fe2+ + H2N-CH-COO•
- CO2
1
R
H2N-CH
•
O2
HO2•
+ H3O+
NH4+ + CHO
R

Figure 7